Journal of Advanced Research 8 (2017) 561–568

Contents lists available at ScienceDirect

Journal of Advanced Research

journal homepage: www.elsevier.com/locate/jare

Original Article

Economical synthesis of silver nanoparticles using leaf extract of *Acalypha hispida* and its application in the detection of Mn(II) ions

R. Sithara [a], P. Selvakumar [a], C. Arun [a], S. Anandan [b], P. Sivashanmugam [a,*]

[a] Department of Chemical Engineering, National Institute of Technology, Tiruchirappalli, Tamil Nadu 620 015, India
[b] Nanomaterials & Solar Energy Conversion Lab, Department of Chemistry, National Institute of Technology, Tiruchirappalli, Tamil Nadu 620 015, India

GRAPHICAL ABSTRACT

ARTICLE INFO

Article history:
Received 10 April 2017
Revised 7 July 2017
Accepted 7 July 2017
Available online 10 July 2017

Keywords:
Acalypha hispida
Silver nanoparticles
TEM
GC–MS
Mn(II) ions
Industrial effluents

ABSTRACT

This study was focused on the synthesis of silver nanoparticles using *Acalypha hispida* leaf extract and the characterization of the particles using UV–Vis spectroscopy, XRD, FT-IR, and TEM. The results showed the formation of silver nanoparticles, crystalline in nature, with an average size of 20–50 nm. The leaf extract components were analyzed with GC–MS and exhibited a high content of Phytol (40.52%), *n*-Hexadecanoic acid (9.67%), 1,2,3-Benzenetriol (7.04%), α-D-Mannofuranoside methyl (6.22%), and D-Allose (4.45%). The optimization and statistical investigation of reaction parameters were studied and maximum yield with suitable properties of silver nanoparticles was obtained at leaf extract volume (0.5 mL), the concentration of silver nitrate (1.75 mM), and reaction temperature (50 °C). The method of detecting Mn^{2+} ions using the colloidal silver nanoparticles was discussed. The minimum and maximum detection limit were found to be 50 and 200 μM of Mn(II) ions, respectively. Thus, the obtained results encourage the use of economical synthesis of silver nanoparticles in the development of nanosensors to detect the pollutants present in industrial effluents.

Introduction

The unique properties of nanoparticles, especially in the size range 1–100 nm, has made nanotechnology the most interesting area of research. The size, shape, and morphology are the crucial

Peer review under responsibility of Cairo University.
* Corresponding author.
E-mail address: psiva@nitt.edu (P. Sivashanmugam).

http://dx.doi.org/10.1016/j.jare.2017.07.001
2090-1232/

parameters deciding the property of nanoparticles [1]. Hence, many studies were conducted in controlling the size and shape of nanoparticles during the synthesis leading to the conclusion of the method of synthesis playing a major role. Though there are many methods of synthesis including chemical and physical methods, the green synthesis of nanoparticles has gained prominence in recent years [2,3].

The green synthesis uses a variety of reducing agents, including cow's milk, plant extract, microbes, and others [4,5]. Among these methods, the usage of green plant extract has acquired significance due to its properties, such as availability of the source, cost effectiveness, and others. This method is also preferred because of the difficulties faced in other methods as an example of requiring aseptic conditions if bacterial or fungal is a reducing agent.

The plant chosen for this study was *Acalypha hispida*, a common flowering evergreen shrub. Till date, no study was reported for the synthesis of silver nanoparticles (AgNPs) using *Acalypha hispida*. Though there are numerous plants reported to be used as reducing agent in literature, the current study was valid as the plant selected for the synthesis of AgNPs was considered to be an ornamental plant earlier. Moreover, the reaction time was noted to be short compared to the time reported in the literature. The presence of capping agents from the plant leaf extract increases the stability and range of application of the nanoparticles. Thus, the use of such plants, rather than medicinal plants, increases the economic stability as well as the feasibility of the project.

Research on the synthesis of AgNPs is an active area due to its wide range of application in the field of medicine, catalysis, and solar energy conversion due to its optical properties [6]. AgNPs are the most used nanoparticles because it is less expensive, easily available and have excellent antibacterial, antifungal, anticancer properties and uses in the field of drug delivery [5,7–10].

Recently, the studies on AgNPs have extended to the detection of ions including Cu^{2+}, Hg^{2+}, Cr^{6+} [11,12] and chemicals such as dopamine was also detected using the impregnated AgNPs [13]. Therefore, this study includes the application of AgNPs in the detection of Mn(II) ions. Manganese is a ubiquitous element in the earth's crust. Though manganese ions are micronutrients, the increase in level can cause adverse effects in both flora and fauna. The major source of manganese ion of anthropogenic activities is from iron and steel plants, though all other metal processing industries have their own role. The natural sources include volcanic eruptions and erosion of the earth's crust also contribute to increasing the pollutants like Mn(II) ions. Manganese is scientifically proven not to be carcinogenic, but the ions can build up in the food chain and cause biomagnification. The prolonged exposure of human to the Mn(II) ions can cause impotence. The determination of manganese ions in public, waste, and industrial effluents are also highly important as higher levels can cause fouling and encrustation of pipelines and process equipment [14,15]. Therefore, this study was mainly focused on the synthesis and characterization of AgNPs and their application as the sensor used for the detection of Mn(II) ions in iron and steel industrial effluents.

Material and methods

Material

Silver nitrate ($AgNO_3$) of analytical grade, methanol (CH_3OH), ethanol (C_2H_5OH) and manganese sulphate ($MnSO_4$) were purchased from Avar Synthesis Pvt. Ltd. (Hyderabad, Andhra Pradesh, India), Loba Chemie Pvt. Ltd. (Mumbai, Maharashtra, India) and Merck Specialities Pvt. Ltd. (Mumbai, Maharashtra, India), respectively. Fresh plant leaves, *Acalypha hispida* (cat's tail), were collected from Malappuram, Kerala, India.

Selection of plant parts

The plant parts required for the synthesis of AgNPs were found out by trial and error method. Various plant parts of different species were tried, including the fruit of *Azadirachta indica* (Neem), leaves of *Adenanthera pavonina* (Manjadi), *Terminalia brellica*, *Prunus dulcis*, and *Acalypha hispida*. Out of these species, the *Acalypha hispida* was chosen for this work based on the efficiency to reduce silver nitrate.

Leaf extract preparation and synthesis of AgNPs

The fresh leaves collected was washed thoroughly in double distilled water. The leaves were then diced into small pieces and 20 g was weighed out, crushed using a mortar and pestle after addition of 100 mL methanol. The mixture was filtered using filter paper followed by Whatman No. 1 filter paper (Wipro GE Healthcare Pvt. Ltd., Chennai, India) and then stored at 4 °C as Methanol Leaf Extract (MLE) for further use. A 0.5 mL MLE was added to a 100 mL conical flask containing 50 mL aqueous solution of 1.75 mM silver nitrate under stirring condition. Then, the color of the reaction mixture changed within 10 min from colorless to reddish-brown, indicating the formation of AgNPs.

Statistical optimization of AgNPs synthesis using SPSS software

The experiments were conducted by varying the parameters viz. concentration of silver nitrate (0.5–2 mM), volume of MLE (0.1–0.7 mL) and reaction temperature (30–70 °C) to evaluate the statistical significant of each parameter on AgNPs synthesis. The obtained values were statistically analyzed using ANOVA apart from the confirmation using SPR peak.

Characterization of AgNPs

The characterization is significant as it helps in understanding the size, shape, and morphology of the synthesized nanoparticles. It also enlightens the idea of AgNPs used for the proposed application. The characterization was carried out using UV–visible spectroscopy, X-ray diffraction (XRD), Transmission electron microscopy (TEM), Fourier Transform-Infrared Spectroscopy (FTIR) for AgNPs and MLE composition was analyzed using gas chromatography-mass spectrometry (GC–MS, PerkinElmer, Bengaluru, Karnataka, India) and identified by library NIST 2005.

In this study, a UV–Visible spectrophotometer (Shimadzu UV-PC Scanning Double Beam, Mumbai, Maharashtra, India) was used to monitor the green synthesis of AgNPs. The respective SPR peaks were recorded between 300 and 500 nm. The reddish brown colloidal liquid was centrifuged (MPW Med. Instruments, Warsaw, Poland) at 10,000 RPM for 30 min to get the powdered nanoparticles, which was then washed thoroughly with double distilled water, followed by washing with 100% ethanol to remove the unwanted organic matter. The resultant was poured into a petri dish and allowed to dry in hot air oven at 45 °C for 12 h. The obtained powdered AgNPs were analyzed using XRD (Rigaku Ultima III XRD, Mumbai, Maharashtra, India) with the 2θ angle noted in the range of 20–80°. Then, the size of AgNPs was calculated using Scherer equation.

The TEM studies were carried out using Jeol/JEM 2100 (Delhi, New Delhi, India) of voltage 200 kV, camera length 80–2000 nm and resolution point: 0.23 nm, Lattice: 0.14 nm. The FT-IR (Proprietary KBr beamsplitter of PerkinElmer/Spectrum 2, Bengaluru, Karnataka, India) was studied in the wavelength range of 8300–350 cm^{-1} to find the functional groups present around the synthesized AgNPs.

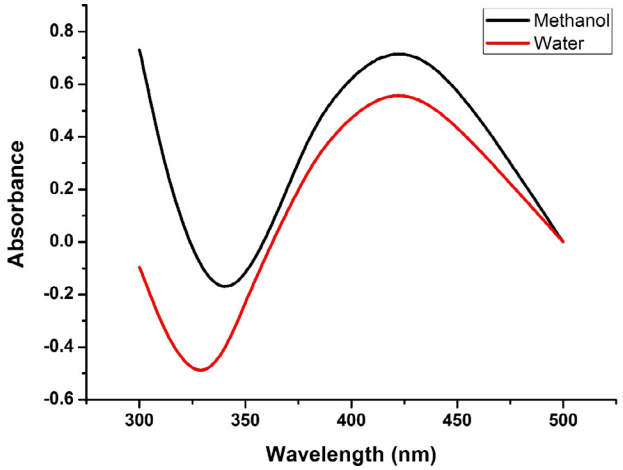

Fig. 1. UV–Visible absorption spectra of synthesized AgNPs.

Stability of AgNPs

The stability of colloidal AgNPs was elucidated through testing the shift in SPR peak with an increase in incubation time (0–30 days).

Colorimetric detection of manganese (II) ions

The colorimetric detection of Manganese (II) ions was performed by the addition of 1 mL of Mn(II) (0–250 μM) to the colloidal solution of volume 2 mL. This was then placed on a magnetic stirrer at atmospheric pressure and room temperature for 10 min and the color transformation was noted followed by acclaiming the SPR peak. The AgNPs-Mn^{2+} complex was centrifuged and analyzed with particle size analyzer (HORIBA Laser Scattering Particle Size Distribution Analyzer LA-960, Bengaluru, Karnataka, India).

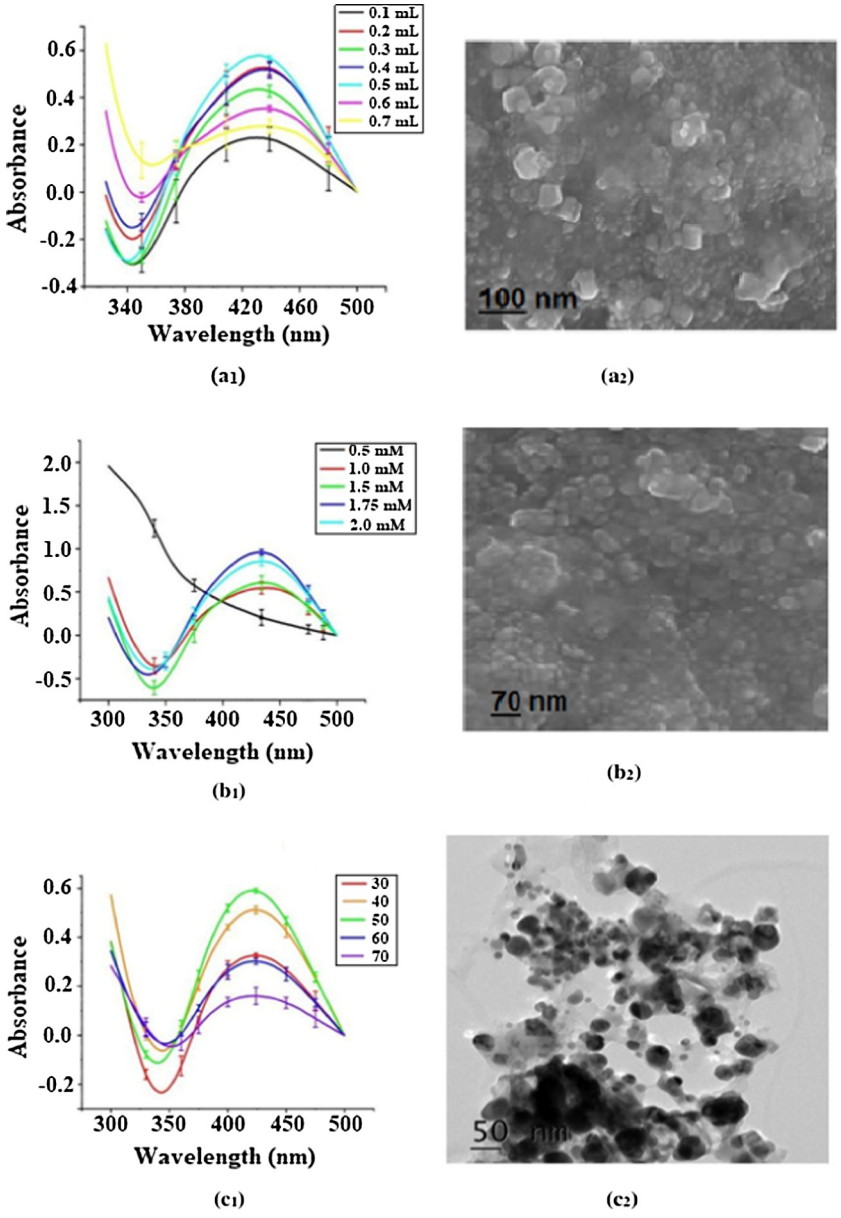

Fig. 2. (a_1) Effect of MLE volume on AgNPs synthesis; (a_2) TEM image of AgNPs at optimum MLE volume; (b_1) effect of $AgNO_3$ concentration on AgNPs synthesis; (b_2) TEM image of AgNPs at optimum MLE volume and $AgNO_3$ concentration; (c_1) effect of reaction temperature on AgNPs synthesis; (c_2) TEM image of AgNPs at optimal conditions.

Table 1
Variables and experimentally observed responses for ANOVA.

Run	Factor A	Factor B	Factor C
1	30	1.75	0.5
2	40	1.75	0.5
3	50	1.75	0.5
4	60	1.75	0.5
5	70	1.75	0.5
6	30	0.5	0.5
7	30	1	0.5
8	30	1.5	0.5
9	30	1.75	0.5
10	30	2	0.5
11	30	1	0.1
12	30	1	0.2
13	30	1	0.3
14	30	1	0.4
15	30	1	0.5
16	30	1	0.6
17	30	1	0.7

A-Temperature (°C), B-$AgNO_3$ concentration (mM), C-MLE volume (mL).

Results and discussion

Synthesis and confirmation of AgNPs

Though there were many studies conducted on the synthesis of AgNPs, the current study is substantial as the plant used was considered as an ornamental plant earlier. In the addition of 0.5 mL of plant extract to 50 mL of 1.75 mM $AgNO_3$ resulted in a color transformation from colorless to lightly brown and then to reddish brown within 10 min. The color change is attributed to the changes in morphology of AgNPs with time. The excitation of surface plasmon vibrations caused by the reduction reaction was studied and then AgNPs formed was confirmed further using UV–Visible spectroscopy, which showed the peak at a wavelength of 424 nm, which is in good agreement with reported literature, where the AgNPs synthesized using *Limonia acidissima* gives a SPR peak at 425 nm [16].

The extraction of compounds from leaves were carried out using two different solvents viz. water and methanol. When AgNPs were synthesized using methanol leaf extract (MLE), the absorbance value was high compared to the value obtained when water leaf extract was used (Fig. 1). It was observed that there was a significant increase in the concentration of AgNPs when the MLE was used due to the effective extraction of reducing components.

Statistical study of reaction parameters

Effect of MLE volume on AgNPs synthesis

The MLE volume varied from 0.1 to 0.7 mL for 50 mL of 1 mM $AgNO_3$ solution at room temperature. The effect of variation in MLE volume on the reduction of $AgNO_3$ is depicted in Fig. 2a1. For lower concentrations of the leaf extract (0.1 and 0.2 mL) predominant color change was observed after 30 min and faster color change and the darker reddish brown color was observed at higher concentrations (0.3–0.5 mL). The value of absorbance was found to increase with increasing MLE concentration and the maximum SPR peak was observed at a wavelength of 424 nm for 0.5 mL of leaf extract. As the leaf extract concentration increases, a number of active biomolecules responsible for the reduction of $AgNO_3$ also increases resulting in an increase of absorbance [4]. The fall in the peak height above 0.5 mL of MLE can be considered due to the presence of components that have not reacted with components of MLE. The TEM image of AgNPs at optimal MLE volume is depicted in Fig. 2a2. Hence, 0.5 mL of MLE is considered as optimum for further studies. Therefore, it is seen that the quantity of MLE required for the reaction is low compared to the volume of extract used in existing literature, where up to 4 mL of extract was used for the reaction [17].

Effect of $AgNO_3$ concentration on AgNPs synthesis

To study the effect of $AgNO_3$ concentration on AgNPs synthesis, the molarity of 50 mL $AgNO_3$ solution varied from 0.5 to 2 mM for 0.5 mL of MLE at room temperature as per the reported methods [18,19]. When using the concentration of 0.5 mM $AgNO_3$, no significant result was obtained. The light brown color was observed at the molarity of 1 and 1.5 mM and darker shades were observed at 1.75 and 2 mM. As observed from Fig. 2b1 the SPR peaks are found to increase with the increase in molarity of $AgNO_3$ concentration till 1.75 mM and then a drop in the height of SPR peak was noticed. Thus, the maximum absorbance was observed at a wavelength of 424 nm for 1.75 mM $AgNO_3$ and this was considered as an optimal value. The size and shape of AgNPs synthesized at the optimal values of MLE volume and concentration of $AgNO_3$ is depicted in Fig. 2b2. This result reveals that the leaf extract of *Acalypha hispida* has the ability to reduce higher concentrations of $AgNO_3$ than the earlier reported plants [20].

Effect of temperature on AgNPs synthesis

The temperature of the reaction mixture (50 mL of 1.75 mM $AgNO_3$ solution and 0.5 mL of MLE) was varied from 30 to 70 °C as suggested in the literature [18]. The variation in absorbance of AgNPs solution with varying temperature is depicted in Fig. 2c1. Temperature was found to alter the rate of reaction significantly. As the temperature was increased up to 50 °C, the time required for color change was decreased, indicating an increase in reaction rate. At the maximum absorbance corresponding to a wavelength of 424 nm, the color change was observed within 10 min at a temperature of 50 °C. However, for temperatures (>50 °C), a drop in SPR peak height was observed, which may be due to degradation of biomolecules present in MLE. Hence, it can be concluded that 50 °C could be the optimal value. The TEM image of AgNPs synthesized at optimal condition is depicted in Fig. 2c2. The above discussed parameters were further statistically analyzed by ANOVA

Table 2
Analysis of variance (ANOVA) for reaction parameters of AgNPs synthesis.

Source	Type III sum of squares	df	Mean square	F	Sig.
Corrected model	2.081	14	0.149	43.428	<0.0001
Intercept	3.724	1	3.724	1088.055	<0.0001
A	0.367	4	0.092	26.813	<0.0001
B	1.080	4	0.270	78.915	<0.0001
C	0.267	6	0.045	13.019	<0.0001
Error	0.123	36	0.003		
Total	13.055	51			
Corrected total	2.204	50			

R Squared = 0.944; Adjusted R Squared = 0.922; A-Effect of temperature of reaction on AgNPs synthesis, B–Effect of $AgNO_3$ concentration on AgNPs synthesis, C–Effect of MLE volume on AgNPs synthesis.

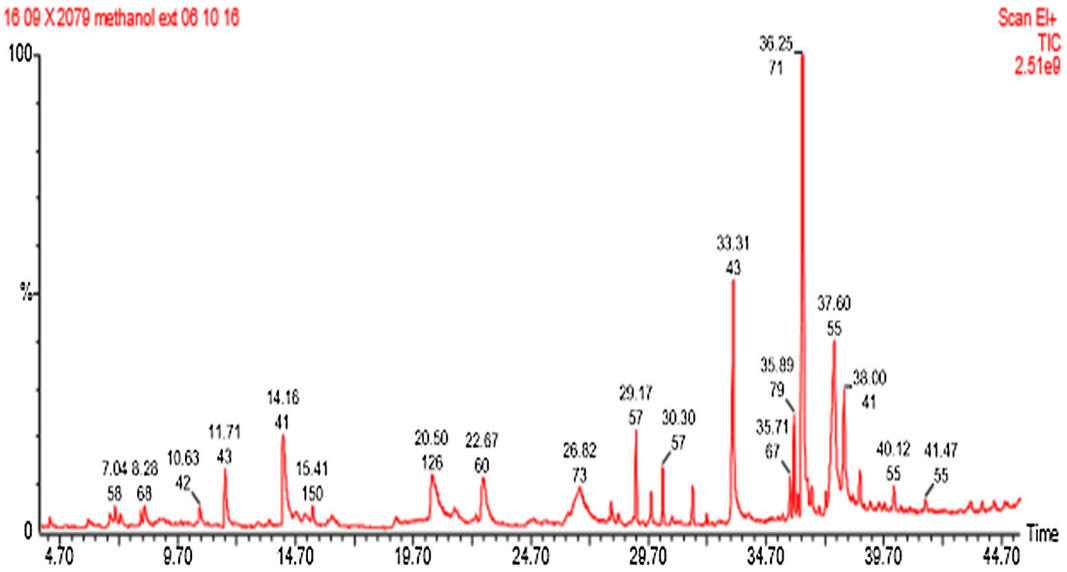

Fig. 3. GC–MS chromatogram of MLE.

Table 3
Components of MLE corresponding with retention time.

Compound name	Retention time (min)
2,4-Dihydroxy-2,5-dimethyl-3(2H)-furan-3-one	7.04
2-Oxabicyclo[3.2.0]hepta-3,6-diene	8.28
Levoglucosenone	10.63
4H-Pyran-4-one, 2,3-dihydro-3,5-dihydroxy-6-methyl-	11.71
2-Furancarboxaldehyde, 5-(hydroxymethyl)-	14.16
2-Methoxy-4-vinylphenol	15.41
1,2,3-Benzenetriol	20.50
D-Allose	22.67
α-d-Mannofuranoside, methyl	26.82
3,7,11,15-Tetramethyl-2-hexadecen-1-ol	29.17
3,7,11,15-Tetramethyl-2-hexadecen-1-ol	30.30
n-Hexadecanoic acid	33.31
9,12-Octadecadienoic acid, methyl ester	35.71
9,12,15-Octadecatrienoic acid, methyl ester, (Z,Z,Z)-	35.89
Phytol	36.25
1,5-Cyclodecadiene, 1,5-dimethyl-8-(1-methylethylidene)-, (E,E)-	37.60
Octadecanoic acid	38.00
Kauran-16-ol	40.12
N-(4-Acetamidophenyl)-1-adamantanecarboxamide	41.47

and the same was presented in Tables 1 and 2. The statistical results revealed that each parameter was statistically significant individually, there is no remarkable effect when they interact.

Analysis of MLE components using GC-MS

The chromatogram of MLE is depicted in Fig. 3 and exhibiting compounds with corresponding retention time (min) are indicated in Table 3. The components existing in abundance may be responsible for the reduction of silver ions to AgNPs. Further, these components act as capping agents to improve the stability of AgNPs as well as the detection capability of Mn^{2+} ions.

Characterization of AgNPs using XRD, TEM, and FTIR

The X-ray Diffraction pattern of synthesized AgNPs is presented in Fig. 4a. The narrow peaks in the pattern indicate the crystalline nature of nanoparticles. The peaks corresponding to 2θ values 38.21°, 44.39°, 64.58°, and 77.8° represent face centered cubic lattice of silver corresponding Miller indices of (1 1 1), (2 0 0), (2 2 0), and (3 1 1). This result was comparable to the standard data of JCPDS No. 04–0783 [21–25]. The average particle size was calculated by Scherrer equation and was found to be in the range of 20–50 nm. Additional peaks were observed at 2θ values 27.8°, 32.2°, 54.8°, and 57.5°, which may correspond to the presence of certain organic compounds present in the extract.

The morphology, size, and, shape of the synthesized AgNPs were determined by TEM. The TEM image of synthesized AgNPs at optimized condition is presented in Fig. 2c2 and it revealed that the synthesized AgNPs are spherical in shape without any aggregates. The obtained results were quite similar to previously reported study [26]. The particle size distribution analysis result showed that the mean diameter of the AgNPs alone was 0.050 μm (Fig. 4b).

FT-IR was performed to identify the bond linkages and functional groups associated with the MLE treated with $AgNO_3$ [27]. Identification of these groups is important to understand its involvement in the reduction process. Fig. 4c represents the FT-IR spectra indicating bands at 3360.42, 3226.91, 1628.49, 1083.15, 810.48, 613.03, and 505.85 cm^{-1}, which are respectively assigned to the stretching vibrations of O—H of carboxylic acids, C—H of aromatic, N—H of amines, C—N of aliphatic amines, C—Cl of alkyl halides, and C=C of alkynes. This result corresponds to the data reported [28], where the functional groups reported were O—H stretching, H-bonded alcohols and phenols, Carbonyl stretching, N—H bond 1° amines corresponding to C—N stretching of the aromatic amino group and C—O stretching alcohols, ethers, and others. The result obtained not only indicates the involvement of MLE in the reduction of $AgNO_3$ but also proves to work as a capping agent for AgNPs.

Stability of synthesized colloidal AgNPs

Stability is a decisive factor for every long-term application of all nanoparticles. In this study, the AgNPs synthesis reaction is very rapid when compared with the other previously reported methods. In earlier studies, the time taken for completion of the reaction was found to be 45 min [29], which led to checking of the stability of colloidal AgNPs. The stability of synthesized AgNPs was performed for an incubation period of 30 days at atmospheric conditions. The

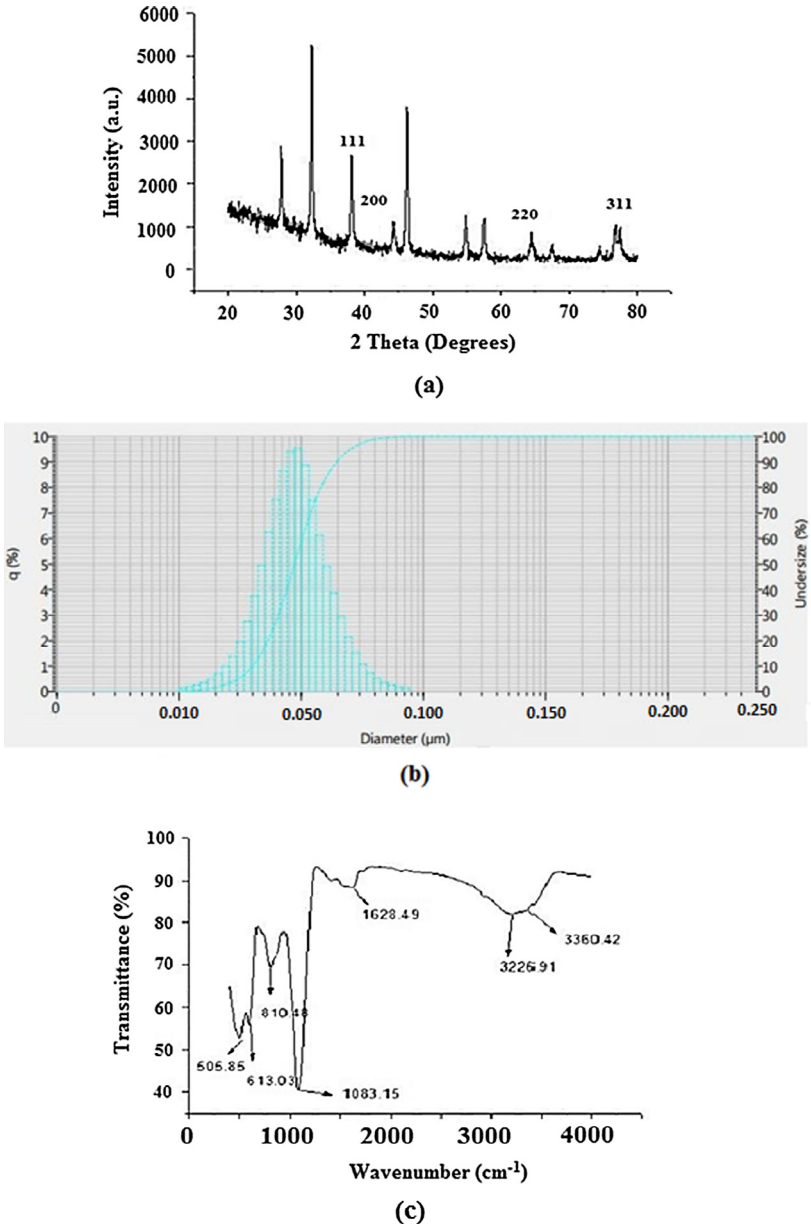

Fig. 4. (a) X-ray diffraction pattern of AgNPs; (b) particle size distribution of AgNPs; (c) FTIR spectra of AgNPs.

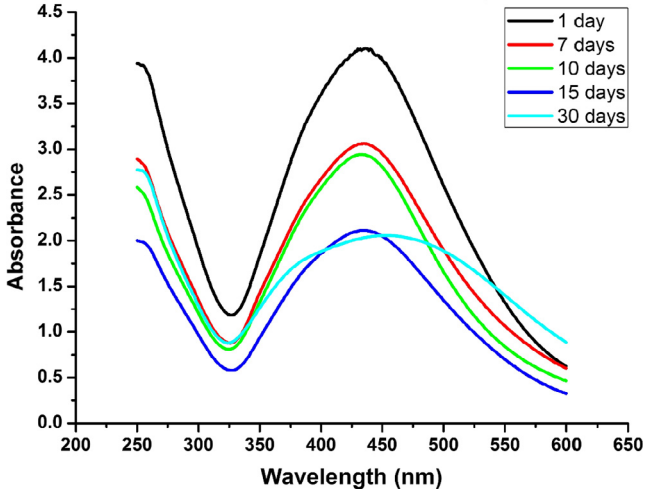

Fig. 5. Stability of AgNPs against incubation time.

SPR peak of AgNPs was recorded at regular time intervals, which is depicted in Fig. 5. It was noted that the peak height was reduced as incubation time was increased. This indicates that the amount of uniformly sized particles was varied in the colloidal solution due to aggregation of nanoparticles. The stability of AgNPs could be increased by using the selective compounds present in leaf extract for the reduction of $AgNO_3$, which act as a stable capping agent.

Colorimetric detection of Mn (II) ions using AgNPs

To confirm, the practical application capability of AgNPs probe prepared from *Acalypha hispida* leaf extract, the concentration of Mn(II) in real wastewater sample (Iron and steel industry effluent) was determined. When the prepared colloidal AgNPs interacted with an aqueous solution of Mn(II) ions for 15 min at room temperature, the result was a colorless liquid with black particles suspended in it, which is depicted in Fig. 6a. This is assumed to be the result of the aggregation of particles. The aggregation in

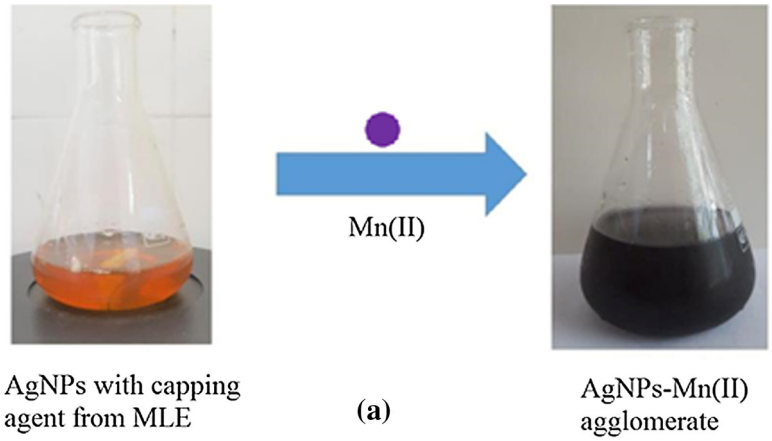

(a)

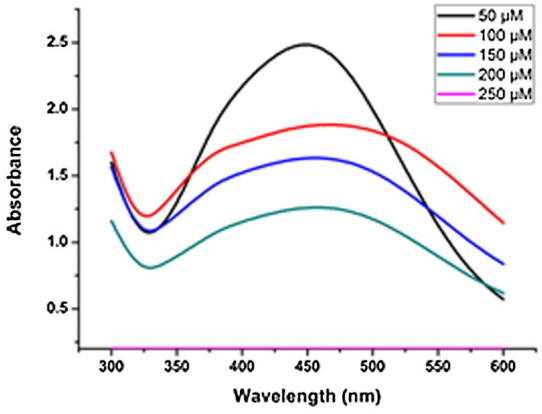

(b)

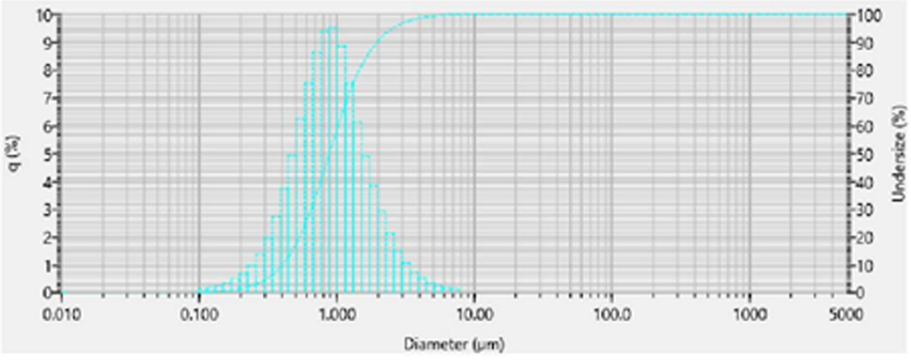

(c)

Fig. 6. (a) Visual observation of aggregation of AgNPs and Mn(II) ions; (b) distorted peaks of colloidal AgNPs interaction with Mn^{2+} ions ; (c) particle size distribution of AgNPs–Mn(II) complex.

different concentrations of Mn(II) ions with the corresponding red shift of the UV–Visible spectra is depicted in Fig. 6b. The colloidal AgNPs were tested with various concentrations (50–250 µM) of Mn(II) ions. It was noted that as the concentration of the Mn(II) ions increased up to 200 µM, the UV–Visible spectral peak was reduced and beyond that, no peaks were observed. Therefore, the lower and maximum detection limit of this method was found to be 50 and 200 µM of Mn (II) ions, respectively. A similar detection mechanism was reported earlier where Cr (III) ions interacted with colloidal AgNPs prepared using *A. occidentale* as reducing agents. There the color change was from brownish black to purple color [12]. Similarly, the Cu(II) ions and Hg(II) ions were detected by colloidal AgNPs synthesized using *Citrullus lanatus* extract [11]. The colloidal AgNPs interacted with other heavy metal ions including iron (Fe^{2+} and Fe^{3+}), chromium (Cr^{3+} and Cr^{6+}), nickel (Ni^{2+}) and zinc (Zn^{2+}) to check if the color change was specifically for Mn(II) ions. Even after incubating the mixture for 48 h at room temperature, there was no visible color change observed and also, no peak distortion was observed in UV–Vis spectrum as in the case of heavy metal cations other than Mn(II) ions. Hence, it can be concluded from the colorimetric method that using AgNPs synthesized from *Acalypha hispida* leaf extract is specific for manganese (II) ions. Thus, this study results demonstrated that the currently designed colorimetric method may be applicable for the detection of Mn (II) in real environmental water samples.

The most common methods existing for the detection of manganese ions are atomic absorption spectroscopy (AAS) and atomic emission spectroscopy (AEDS). In AAS, the sample was first

aspirated into flame until an element was atomized and the ground state atomic vapor was able to absorb monochromatic radiations. A photoelectric detector measures the intensity of radiation absorbed at 279.5 nm. Similar complex steps exist for AES also. The other existing detection techniques are mass spectrometry, neutron activation analysis, and X-ray fluorimetry [30]. The main demerit of all these methods is that they do not distinguish between the oxidation state of manganese ions, unlike the colorimetric detection which exclusively detections Mn(II) ions.

Possible mechanism of colorimetric detection

On addition of colloidal AgNPs solution to Mn(II) ions, it was observed that the color of the solution changes from reddish brown to colorless with suspended black particles. This is because of the receptor-ligand interaction between the capping agent produced from the MLE on AgNPs and the Mn(II) ions which cause the particles to aggregate. The particle size analysis result showed that the mean diameter of the AgNPs–Mn^{2+} complex was 1.08 μm (Fig. 6c). Since there were no such physical changes observed in the case of other ions tested, it can be assumed that the aggregation is mainly due to chelation of Mn(II) ions with the capping agents.

Conclusions

Green synthesis of the nanoparticle is a promising technology, which is eco-friendly and economical. The SPR peaks revealed the particles present is in nanoscale. Further, the size, shape, and morphology were investigated with XRD and TEM, which revealed that the size of particles was 20–50 nm. The stability of the nanomaterial was tested with SPR peaks. The functional groups present as capping agent from the plant extract were discovered from FT-IR results. The effect of parameters was studied with ANOVA approach employing the software SPSS v.21, which proved the effect of parameters individually on the synthesis. Application of results of using the synthesized nanoparticles to detect very low concentrations of range Mn^{2+} ions in waste water in this study is highly encouraging, revealing that the synthesized AgNPs nanoparticle using *Acalypha hispida* extract can be used successfully for the detection of Mn^{2+} in industrial effluents.

Conflict of interest

The authors declared no conflict of interest.

Compliance with Ethics Requirements

This article does not contain any studies with human or animal subjects.

Funding

Authors are thankful to DST, India for the sanction of Water Technology Initiative (WTI) research grant (DST/TM/WTI/2k16/258(G) dated 21/02/2017) and TNSCST/SPS/AR/2016–17/1376 (Project Code No-CHE – 01) dt. 10/04/2017 for providing financial support for this project work.

References

[1] Nilesh SP, Raman PY. A simple biogenic method for the synthesis of silver nanoparticles using *Syngonium podophyllum*, an ornamental plant. MGM J Med Sci 2016;3(3):111–5.
[2] Ahmed S, Ahmad M, Swami BL, Ikram S. A review on plants extract mediated synthesis of silver nanoparticles for antimicrobial applications: a green expertise. J Adv Res 2016;7(1):17–28.
[3] Kholoud MM, Abou El-Nour, Ala'a Eftaiha, Abdulrhman Al-Warthan, Reda AA Ammar. Synthesis and applications of silver nanoparticles. Arab J Chem 2010; 3: 135–140.
[4] Chinnappan S, Kandasamy S, Muthusamy G, Balakrishnan S, Arumugam S, Murugesan S, et al. *Acorus calamus* rhizome extract mediated biosynthesis of silver nanoparticles and their bactericidal activity against human pathogens. J Genet Eng Biotechnol 2015;13(2):93–9.
[5] Selvakumar P, Viveka S, Prakash S, Jasminebeaula S, Uloganathan R. Antimicrobial activity of extracellularly synthesized silver nanoparticles from marine derived *Streptomyces rochei*. Int J Pharm Bio Sci 2012;3(3):188–97.
[6] Hussain JI, Kumar S, Hashmi AA, Khan Z. Silver nanoparticles: preparation, characterization, and kinetics. Adv Mater Lett 2011;2(3):188–94.
[7] Kalaiselvi M, Subbaiya R, Masilamani Selvam. Synthesis and characterization of silver nanoparticles from leaf extract of Parthenium hysterophorus and its antibacterial and antioxidant activity. Int J Curr Microbiol Appl Sci 2013;2(6):220–7.
[8] Khalil KA, Fouad H, Elsarnagawy T, Almajhdi FN. Preparation and characterization of electrospun PLGA/silver composite nanofibers for biomedical applications. Int J Electrochem Sci 2013;8(3):3483–93.
[9] Patricia LN, JianFei W, Edward ET, Robert EB. Anti-inflammatory activity of nanocrystalline silver-derived solutions in porcine contact dermatitis. J Inflamm (Lond) 2013;7(13):1–20.
[10] Ahmad N, Sharma S. Green synthesis of silver nanoparticles using extracts of *Ananas comosus*. Green Sustain Chem 2012;2:141–7.
[11] Maiti S, Barman G, Konar LahaJ. Detection of heavy metals (Cu^{2+}, Hg^{2+}) by biosynthesized silver nanoparticles. Appl Nanosci 2016;6(4):529–38.
[12] Balavigneswaran CK, Sujin Jeba Kumar T, Moses Packiaraj R, Prakash S. Rapid detection of Cr(VI) by AgNPs probe produced by *Anacardium occidentale* fresh leaf extracts. Appl Nanosci 2014;4(3):367–78.
[13] Nivedhini Iswarya C, Kiruba Daniel SCG, Sivakumar M. Studies on L-Histidine capped Ag and Au nanoparticles for dopamine detection. Mater Sci Eng C 2017;75:393–401.
[14] Joselow MM, Tobias E, Koehler R, Coleman S, Bogden J, Gause D. Manganese pollution in the city environment and its relationship to traffic density. Am J Public Health 1978;68(6):557–60.
[15] Van Staden JF, Kluever LG. Determination of manganese in natural water and effluent streams using a solid-phase lead(IV) dioxide reactor in a flow-injection system. Anal Chim Acta 1997;350(1–2):15–20.
[16] Chandra Sekhar E, Krishna Rao KSV, Madhusudana Rao K, Pradeep Kumar S. A green approach to synthesize controllable silver nanostructures from *Limonia acidissima* for inactivation of pathogenic bacteria. Cogent Chem 2016;2:1–14.
[17] Ahmed S, Ikram S. Silver nanoparticles: one pot green synthesis using *Terminalia arjuna* extract for biological application. J Nanomed Nanotechnol 2015;6(4):309.
[18] Iravani S, Korbekandi H, Mirmohammadi SV, Zolfaghari B. Synthesis of silver nanoparticles: chemical, physical and biological methods. Res Pharm Sci 2014;9(6):385–406.
[19] Ashok Kumar D, Palanichamy V, Roopan SM. Green synthesis of silver nanoparticles using *Alternanthera dentata* leaf extract at room temperature and their antimicrobial activity. Spectrochim Acta A Mol Biomol Spectrosc 2014;127:168–71.
[20] Christensen L, Vivekanandhan S, Misra M, Mohanty AK. Biosynthesis of silver nanoparticles using *Murraya koenigii* (curry leaf): an investigation on the effect of broth concentration in reduction mechanism and particle size. Adv Mater Lett 2011;2(6):429–34.
[21] Priyanka T, Khandelwal M, Priyanka S. Statistically optimized synthesis of silver nanocubes from peel extracts of *Citrus limetta* and potential application in waste water treatment. J Microbial Biochem Technol 2014;S4:004. doi: http://dx.doi.org/10.4172/1948-5948.S4-004.
[22] Kaviya S, Santhanalakshmi J, Viswanathan B. Green synthesis of silver nanoparticles using *Polyalthia longifolia* leaf extract along with D-Sorbitol: Study of antibacterial activity. J Nanotech 2011. http://dx.doi.org/10.1155/2011/152970.
[23] Manal AA, Awatif AH, Khalid MOO, Dalia FAE, Nada EE, Lamia AA, et al. Silver nanoparticles biogenic synthesized using an orange peel extract and their use as an orange peel extract and their use as an antibacterial agent. Int J Phys Sci 2014;9(3):34–40.
[24] Shiraishi Y, Toshimma N. Oxidation of ethylene catalysed by colloidal dispersions of poly (sodium acrylate) - protected silver nanoclusters. Colloids Surf A 2000;169:59–66.
[25] Sharverdi AR, Mianaeian S, Shahverdi HR, Jamalifar H, Nohi AA. Rapid synthesis of silver nanoparticles using culture supernatants of enterobacteria: a novel biological approach. Process Biochem 2007;2:919–23.
[26] Loo YY, Chieng BW, Nishibuchi M, Radu S. Synthesis of silver nanoparticles by using tea leaf extract from *Camellia sinensis*. Int J Nanomed 2012;7:4263–7.
[27] Das J, Velusamy P. Biogenic synthesis of antifungal silver nanoparticles using aqueous stem extract of banana. Nano Biomed Eng 2013;5(1):34–8.
[28] Shanmuga Praba P, Vasantha VS, Jeyasundari J, Brightson Arul Jacob Y. Synthesis of plant-mediated silver nanoparticles using *Ficus microcarpa* leaf extract and evaluation of their antibacterial activities. Eur Chem Bull 2015;4(3):117–20.
[29] Mohan Kumar K, Sinha M, Mandal BK, Ghosh AR, Siva Kumar K, Reddy PS. Green synthesis of silver nanoparticles using *Terminalia chebula* extract at room temperature and their antimicrobial studies. Spectrochim Acta A Mol Biomol Spectrosc 2012;91:228–33.
[30] Williams M, Todd GD, Roney N, et al. Toxicological profile for manganese. Atlanta (GA): Agency for Toxic Substances and Disease Registry (US); 2012 Analytical methods. <https://www.ncbi.nlm.nih.gov/books/NBK158867/>.